Pergamon

SCIENCE DIRECT®

Tetrahedron 59 (2003) 10187–10193

TETRAHEDRON

1,5-Type nonbonded O···S and S···S interactions in (acylimino) and (thioacylimino)benzothiazoline systems. Crystal structures and theoretical calculations

Emerson Meyer,[a] Antonio C. Joussef,[a] Hugo Gallardo,[a,*] Adailton J. Bortoluzzi[a] and Ricardo L. Longo[b]

[a]*Departamento de Química, Universidade Federal de Santa Catarina, 88040-900 Florianópolis, SC, Brazil*
[b]*Departamento de Química Fundamental, Universidade Federal de Pernambuco, 50740-540 Recife, PE, Brazil*

Received 6 August 2003; revised 23 October 2003; accepted 23 October 2003

Abstract—Intramolecular nonbonded interactions have been observed in the crystalline structures of 6-ethoxy-2-trifluoroacetylimino-benzothiazoline (**4**) (S···O close contact) and 6-ethoxy-2-trifluorothioacetyliminobenzothiazoline (**5**) (S···S close contact). Density functional B3LYP/6-311G** calculations were performed for all conformers and tautomers of **4** and **5** in order to explain the preference for the S···O and S···S close contact structures. The calculations agree with the observed crystallographic structures only when solvent effects are included via a continuum model, thus showing the importance of the solvent effects to establish the correct relative energies.

1. Introduction

The possibility of the establishment of noncovalent attractive interactions involving chalcogen atoms from one side and oxygen or nitrogen atoms from the other side has long been recognized.[1–4] These interactions play an important role in governing properties like spectroscopic behavior and chemical reactivity.

Several examples of organosulfur compounds are known, whose conformations, geometries and biological activity, are influenced by intramolecular nonbonded sulfur–oxygen, sulfur–nitrogen or sulfur–sulfur interactions.[5–12] In these molecules, the S···O, S···N and S···S nonbonded distances are significantly shorter than the sum of the corresponding van der Waals radii (3.32, 3.35 and 3.60 Å, respectively).

In medicinal chemistry, special attention has been paid to the influence of such nonbonded interactions on the design of new drug candidates.[13–15] Recently, Nagao and his collaborators studied the intramolecular nonbonded 1,5-type S···O and S···S interactions in (acylimino) and (thioacylimino)thiadiazoline derivatives and observed that in contrast with the oxadiazoline analogues (where the close contact O···O is weaker) the S···O nonbonded interaction plays a decisive role in their affinity to the AT_1 receptor in compounds tested as AII receptor antagonists (Fig. 1).[10,11,15] On the basis of their X-ray analyses, the nonbonded atom distances between the sulfur atom of the thiadiazoline ring and the oxygen (**1**) and sulfur (**2**) atoms of the acyl moiety were found to be 2.648(3) and 2.905(1) Å, respectively (as indicated by dashed lines in Figure 1).

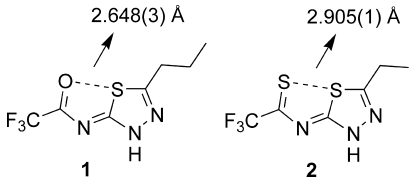

Figure 1. S···O and S···S close-contact systems.

In the course of our studies involving the 2-amino-benzothiazole system as the heterocyclic moiety in the synthesis of new models for AII receptor antagonists, we speculated that the same kind of intramolecular nonbonded 1,5-type S···O and S···S interactions could be occurring in their acylimino derivatives. In order to evaluate the (acylimino) and (thioacylimino)benzothiazoline moieties as mimic-fused heterocycles (Fig. 2), we investigated the intramolecular noncovalent S···O and S···S interactions of two simplified model compounds through their X-ray crystallographic analyses and density functional B3LYP/6-311G** calculations.

Keywords: close contact; benzothiazoles; X-ray crystal structures.
* Corresponding author. Tel.: +55-483319544; fax: +55-483319711; e-mail: hugo@qmc.ufsc.br

0040–4020/$ - see front matter © 2003 Elsevier Ltd. All rights reserved.
doi:10.1016/j.tet.2003.10.066

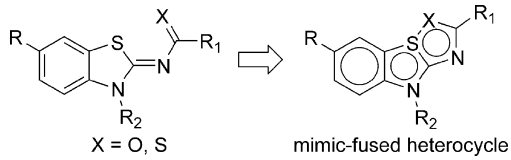

Figure 2. (Acylimino) and (thioacylimino)benzothiazoline as mimic-fused heterocycles.

2. Results and discussion

2.1. Synthesis

The model compound 6-ethoxy-2-trifluoroacetyliminobenzothiazoline (**4**) was prepared by trifluoroacetylation of 2-amino-6-ethoxybenzothiazole (**3**) with trifluoroacetic anhydride, which was converted into the model compound 6-ethoxy-2-trifluorothioacetyliminobenzothiazoline (**5**) through treatment with Lawesson's reagent[16] as shown in Scheme 1.

Table 1. Summary of the X-ray crystallographic analyses of compounds **4** and **5**

	4	**5**
Empirical formula	$C_{11}H_9F_3N_2O_2S$	$C_{11}H_9F_3N_2OS_2{\cdot}C_3H_8O$
Formula weight	290.26	366.42
Crystal system	Monoclinic	Triclinic
Space group	$P2_1/c$	$P\bar{1}$
a (Å)	13.582(3)	8.038(1)
b (Å)	10.584(2)	8.932(1)
c (Å)	8.585(2)	14.721(1)
α (°)		79.22(1)
β (°)	103.53(3)	75.64(1)
γ (°)		66.29(1)
Volume (Å^3)	1199.9(4)	876.5(2)
Temperature (K)	293(2)	293(2)
Z	4	2
μ (mm^{-1})	0.308	0.341
$R_1[I>2\sigma(I)]$, wR_2 (all data)	0.0359, 0.1027	0.0502, 0.1474
GOF	1.054	1.037

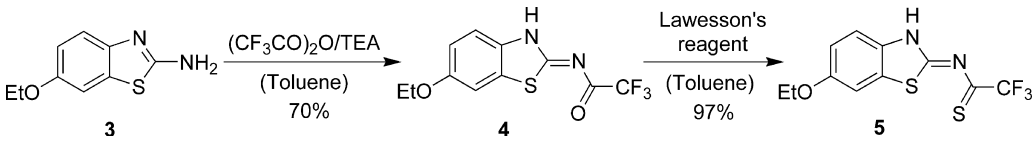

Scheme 1.

2.2. Crystallographic studies

Single crystals suitable for X-ray analysis of the two model compounds (**4** and **5**) were obtained by crystallization from ethanol/water and 2-propanol, respectively.

The X-ray crystallographic data for **4** and **5** are summarized in Table 1. The thermal ellipsoid plots are shown in Figure 3. The computer-generated drawings of the crystal structures of the two model compounds are shown in Figures 4 and 5. Selected atom distances, bond angles and torsion angles of **4** and **5** are listed in Table 2.

In comparison with the model of Nagao and collaborators, the acyliminothiadiazoline **1**, which shows a remarkable S···O close contact (2.648(3) Å) in addition to an essentially planar arrangement between the thiadiazole ring and the acyl moiety, the model compound **4** presents basically the same characteristics.

As indicated in the computer-generated drawing of the crystal structure of **4** (Fig. 4), the nonbonded distance between the sulfur atom of the benzothiazoline ring and the carbonyl oxygen of the acyl moiety was found to be 2.691(2) Å, which implies a significant close contact. A result of this nonbonded interaction is the planarity of the O1–C11–N2–C1–S1 moiety observed in **4** (see torsion angles, Table 2). It is worth noting that the great similarity of the bond lengths C11–N2 and N2–C1 and bond angles O1–C11–N2 and N2–C1–S1 indicates the existence of a quasi ring system (O1–C11–N2–C1–S1), characterizing what Nagao called a 'mimic-fused heterocycle'.

With respect to the thioacetylimino model compound **5**, a remarkable S···S close contact of the 1,5-type was found (3.001(1) Å between S1 and S2) (Fig. 5). By virtue of this intramolecular interaction, the benzothiazoline ring and the thioacetyl moiety adopt, similarly to **4**, an almost planar conformation (see torsion angles, Table 2), with a mean deviation from the plane of only 0.019°. Additionally, the bond angles N2–C1–S1 and N2–C11–S2 are exactly the same and the bond lengths of C1–N2 and N2–C11 are quite

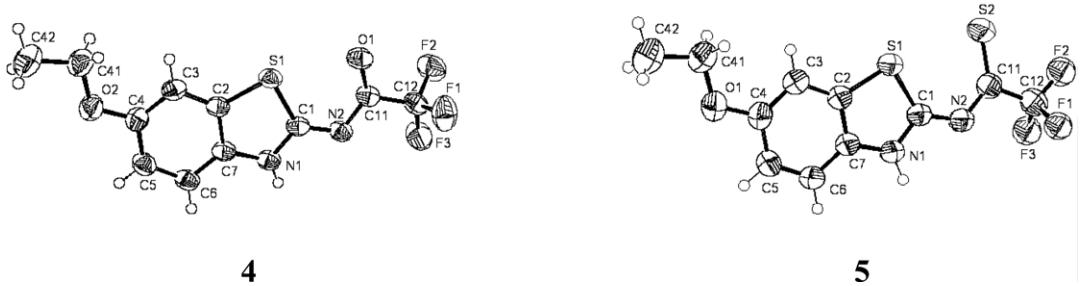

Figure 3. Thermal ellipsoid plot of **4** and **5** showing the atom labeling scheme. Displacement ellipsoids are shown at the 40% probability level. The H atoms are shown with arbitrary size.

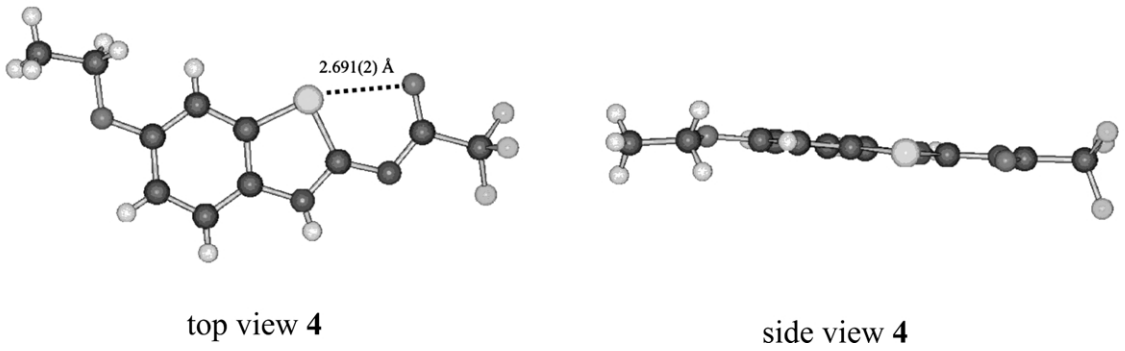

Figure 4. Computer-generated drawings of the model compound **4** derived from the X-ray coordinates. Dotted lines emphasize the S···O close contact.

Figure 5. Computer-generated drawings of the model compound **5** derived from the X-ray coordinates. Dotted lines emphasize the S···S close contact.

Table 2. Selected atom distances, bond angles and torsion angles of compounds **4** and **5**, and B3LYP/6-311G** calculated values in ethanol for isomers **7** and **11**

Benzothiazoline **4**				Benzothiazoline **5**			
	X-Ray	**7**	**11**		X-Ray	**7**	**11**
Atom distances (Å)							
S1–O1	2.691(2)	2.736	2.864	S1–S2	3.001(1)	3.086	3.181
S1–C1	1.743(2)	1.775	1.773	S1–C1	1.746(4)	1.772	1.771
C1–N2	1.329(3)	1.319	1.392	C1–N2	1.336(4)	1.322	1.390
N2–C11	1.327(3)	1.346	1.355	N2–C11	1.318(4)	1.327	1.340
C11–O1	1.238(3)	1.226	1.213	C11–S2	1.659(4)	1.672	1.655
Bond angles (°)							
S1–C1–N2	128.50(16)	128.1	122.5	S1–C1–N2	130.4(3)	129.8	125.2
C1–N2–C11	116.85(19)	118.0	125.8	C1–N2–C11	122.1(3)	124.3	130.3
N2–C11–O1	129.4(2)	129.4	126.1	N2–C11–S2	130.4(3)	130.8	128.2
C1–S1–C2	90.69(10)	90.4	87.5	C1–S1–C2	90.37(16)	90.3	87.5
Torsion angles (°)							
O1–C11–N2–C1	2.5(3)	0.5	1.1	S2–C11–N2–C1	1.6(6)	1.9	0.6
S1–C1–N2–C11	1.8(3)	0.6	0.5	S1–C1–N2–C11	2.7(6)	1.7	0.4

similar for **5**, indicating the presence of a quasi ring system promoted by the attractive S···S interaction.

In considering the potential of **4** and **5** for rotational, geometrical and tautomeric isomerism and based on the above results, we conclude that the nonbonded interactions play a fundamental role in determining the observed structural features of **4** and **5**.

2.3. Computational studies

In order to clarify some aspects of the structural preferences of **4** and **5** we performed density functional B3LYP/6-311G** calculations on all tautomers and conformers presented in Scheme 2. The initial experiments in the gas phase and with C_s symmetry (planar) structures, indicated that only isomers **7**, **8** and **11** were energetically relevant according to the results which are summarized in Table 3.

It should be noted that the B3LYP/aug-cc-pVTZ and B3LYP/6-31G* present an average error of 21.7 and 10.9 kJ/mol for the atomization energies of molecules of the G2 group,[17] so the average error of the B3LYP/6-311G** approach should be close to 12 kJ/mol. As a result, it would seem that this approach lacks the precision to distinguish the **7**, **8** and **11** isomers in Scheme 2 and Table 3. However, for energy differences between similar systems, the error cancellations should improve the performance of the ab initio methods, where the average errors for the conformers relative energies of the HF/TZP,

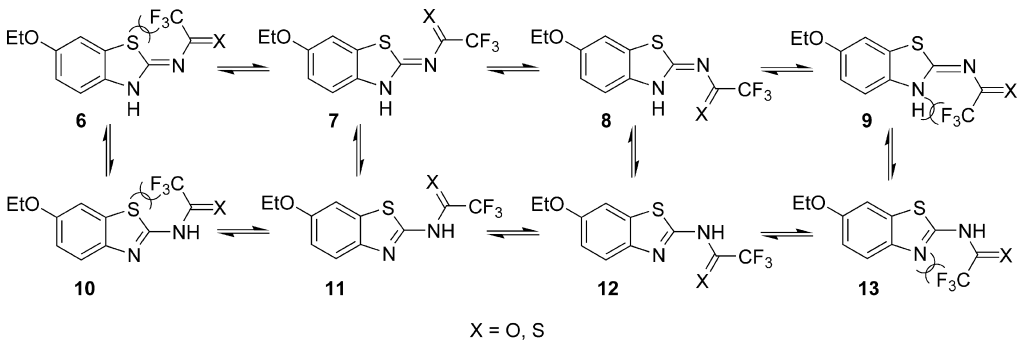

Scheme 2.

MP2/TZP, LSDA/TZP and BP86/TZP are 2.1, 1.7, 2.5 and 1.2 kJ/mol, respectively.[18] We should expect a similar or even better precision for the B3LYP/6-311G** and similar errors for the energy differences between of the tautomers. Thus, the B3LYP/6-311G** approach is adequate for the analysis presented in Tables 3–5. In addition, from Table 3, the inclusion of the solvent effects via the PCM continuum model (ethanol: dielectric constant, ϵ=24.55) usually increases the energy differences between the **7**, **8** and **11** isomers.

Table 3. Relative gas phase and ethanol medium (PCM with gas phase geometry) energies of the isomers **6**–**13** at the B3LYP/6-311G** level

Isomer	Relative energy (kJ/mol)			
	X=O		X=S	
	Gas phase	Ethanol	Gas phase	Ethanol
6	57.5	50.4	51.2	53.3
7	6.3	0.0	4.9	0.0
8	3.4	11.1	0.0	4.7
9	59.0	64.7	52.9	72.2
10	32.8	34.3	28.9	36.5
11	0.0	1.6	3.0	11.9
12	26.7	25.9	28.4	26.0
13	32.6	32.9	32.7	34.7

Table 4. Relative energies of isomers **7**, **8** and **11** at the B3LYP/6-311G** level in solution

Isomer	Relative energy (kJ/mol)			
	X=O		X=S	
	Ethanol	Chlorobenzene	Ethanol	Chlorobenzene
7	0.0	0.0	0.0	0.0
8	13.1	2.9	11.2	2.3
11	12.1	2.8	13.1	5.0

Table 5. Relative gas phase energies of isomers **6**–**13** with the $-CH_3$ replacing the $-CF_3$ group at the B3LYP/6-311G** level

Isomer	Relative energy (kJ/mol)	
	X=O	X=S
6-CH_3	66.1	52.8
7-CH_3	18.2	13.5
8-CH_3	14.1	5.2
9-CH_3	82.8	70.9
10-CH_3	20.5	8.6
11-CH_3	0.0	0.0
12-CH_3	33.0	31.1
13-CH_3	12.5	3.1

It is also clear from the results in Table 3 that the calculated relative energies of the isomers do not correlate with the observed X-ray structures. Thus, assuming that the isomers are in equilibrium it is clear that the most stable isomer in solution would be that observed in the crystalline state, so we have performed the geometry optimization of isomers **7**, **8** and **11** in ethanol (dielectric constant, ϵ=24.55) using the PCM continuum model. The relative energies of these isomers are presented in Table 4 along with the results calculated with chlorobenzene (ϵ=5.62) as the solvent. As can be observed from the results in Table 4, the solvent has an important effect on the relative stabilities of the isomers, which becomes more significant as the dielectric constant of the solvent increases. It is also clear that the solvent is responsible for stabilizing isomer **7** in solution, which is then observed in the crystal. Considering that the crystalline structure for X=O (**4**) is obtained from an ethanol/water solution, which should have a larger dielectric constant than pure ethanol, the trends observed in Table 4 suggest that the energy differences between isomer **7** and the others should become greater. In the case of X=O (**5**), where the solvent is 2-propanol, which has a dielectric constant (ϵ=18.3) slightly smaller than ethanol, but larger than chlorobenzene, it is still expected that isomer **7** would be found in the crystal. However, as noted in the crystallographic section, the loss of the solvent is quite important for the stability of the crystal, which might be related to the lesser energy differences between isomer **7** and the others, when a solvent with a smaller dielectric constant is used. It should be noted that the specific interactions, particularly those of hydrogen bonds, between solute and solvent are not taken into account, since they are expected to be approximately the same for isomers **7**, **8** and **11** due to their structural similarities. In addition, the energy differences between these isomers and the others are so great that it is not worth investing computational resources for the simulation of the solvent effects via a discrete model, that which should be performed by Monte Carlo or molecular dynamics simulations[19,20] that would also require the solute-solvent interaction potential energy function.

Regarding the calculated structural parameters for **4** and **5**, the results presented in Table 2 do show a good agreement with the crystallographic analyses, mainly for bond angles

and for the nonbonded distances S···O and S···S. It should be noted that tautomers **7** and **11** are very similar, and they might not be distinguished in the X-ray crystallographic studies. However, a comparison of the calculated molecular parameters of **7** and **11** presented in Table 2 revealed significant differences mainly for S···O and S···S non-bonded distances and for bond angles, and a much closer agreement with the crystallographic structure was obtained with the calculated structure of **7**.

In order to obtain a better understanding of the origin of the close-contact in isomer **7**, we performed B3LYP/6-311G** calculations of all isomers in Scheme 2, replacing the $-CF_3$ group with a $-CH_3$. The relative energy results for the optimized geometries in the gas phase are presented in Table 5.

For X=O the energy differences between the most stable isomer (**11**) and the others increase significantly when compared to the relative energies for the $-CF_3$ group. On the other hand for X=S the relative energies are smaller and all isomers become important, except isomers **6**, **9** and **12**. These results indicate that the nature of the substituent group at the (thio)keto position is important, if not determinant, for the relative stabilities of the isomers and consequently for the close-contact structures. These results also suggest that the steric and electrostatic effects might be important for explaining the relative stabilities of these isomers. Thus, we present in Table 6 the relative, van der Waals and electrostatic energy contributions to the total energy of the isomers calculated with the molecular mechanics (MM2) method[21] for the B3LYP/6-311G** gas phase geometries.

Table 6. Relative (ΔE), van der Waals (vdW) and electrostatic (elect) energies (kJ/mol) of the isomers calculated with the MM+ method with the B3LYP/6-311G** gas phase structures

Isomer	X=O			X=S		
	ΔE	vdW	elect	ΔE	vdW	elect
6	68.6	25.9	65.7	24.7	26.8	−20.5
7	76.4	38.9	76.6	15.5	38.9	−22.2
8	50.2	30.1	54.8	0.0	28.9	−28.0
9	56.5	20.1	64.0	1.7	20.5	−32.6
10	15.1	24.7	6.7	15.9	26.3	−31.0
11	0.0	29.3	8.8	11.3	29.7	−29.7
12	4.6	21.7	14.2	18.0	22.2	−26.8
13	9.2	20.5	10.0	10.9	21.3	−25.9

Although the geometries were not optimized at the MM2 level, the relative energies of the isomers correlate qualitatively with the B3LYP/6-311G** results. However, the van der Waals and electrostatic contributions correlate even better with the relative stability of the isomers, thus showing that the close-contact structures are determined by the steric and electrostatic interactions between the (thio)keto substitent and the sulfur atom at the hetero cycle. A Mulliken bonding analysis of the most stable isomers (**7**, **8** and **11**) is presented in Figure 6. It can be clearly observed that the bonding interactions between the S···O and S···S close-contact atoms are very small and do not correlate with the relative stabilities of these isomers, thus corroborating the assumption that their stabilities are determined by non-bonding interactions.

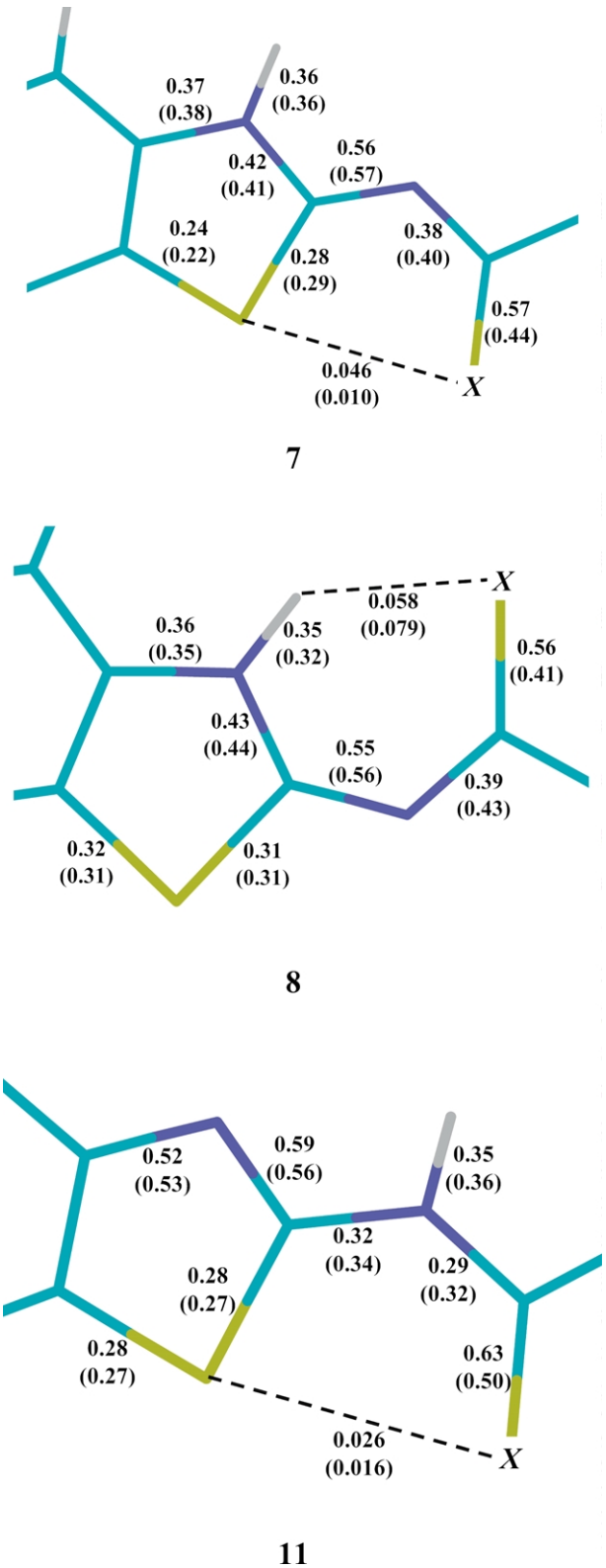

Figure 6. Mulliken bonding analysis for the isomers **7**, **8** and **11** of **4** and **5** (in parenthesis).

3. Conclusion

The crystallographic analysis demonstrated the existence of remarkable nonbonded 1,5-type interactions in the 6-ethoxy-2-trifluoro acetyliminobenzothiazoline (**4**) (S···O

close contact) and in the 6-ethoxy-2-trifluorothioacetylimino-benzothiazoline (**5**) (S···S close contact). In both compounds the X-ray crystallographic analysis suggests the formation of quasi ring systems. DFT-B3LYP/6-311G** calculations revealed that in the gas phase the preferred isomer does not correspond to the S···S close contact structure **5** and the most stable isomer of **4** presents an S···O close contact, although, the distance is ca. 0.2 Å longer than the crystallographic one. However, when the solvent effects are included via a continuum model, isomer **7**, the isomer that presents the S···X close contact, becomes the most stable, in complete agreement with the observed X-ray structures. In addition, it can be expected that other isomers of **4** or **5** could be crystallized if the dielectric constant of the solution is properly decreased or if the (thio)keto substitent is replace by a less bulky group such as $-CH_3$ or $-H$.

In this regard, acylimino and thioacyliminobenzothiazoline systems proved to be promising in the design of new bioactive molecules. The synthesis of potential AII receptor antagonists incorporating (acylimino) and (thioacylimino)-benzothiazoline moieties are in progress in our laboratory.

4. Experimental

4.1. Synthesis

Melting points were measured on a Kofler hot-stage apparatus (Microquímica APF-301) and are uncorrected. IR spectra were obtained with a Perkin–Elmer Model 16 PC-FTIR spectrophotometer. ^{1}H NMR spectra were determined on a Bruker AW-200 (200 MHz) instrument, with tetramethylsilane (TMS) as the internal standard. Elemental analyses were performed on a Perkin–Elmer 2400 instrument. 2-Amino-6-ethoxybenzothiazole (**3**) was purchased from Aldrich Chemical Co. Ltd, and used as received.

4.1.1. 6-Ethoxy-2-trifluoroacetyliminobenzothiazoline (4). Trifluoroacetic anhydride (2.40 mL, 17.0 mmol) was added dropwise to a stirred and cooled (0°C) suspension of 2-amino-6-ethoxybenzothiazole (**3**) (3.00 g, 15.4 mmol) and triethylamine (2.20 mL, 16.2 mmol) in toluene (50 mL). The cooling bath was removed and stirring was continued overnight at room temperature (25°C). The reaction mixture was poured into water (50 mL) and extracted with ethyl acetate (2×20 mL). The organic layer was washed with water (3×20 mL), dried ($MgSO_4$) and evaporated to afford the product (**4**) (3.14 g, 70%) as a pale orange solid. Mp 203–204°C (EtOH/H_2O). (Found: C, 45.46; H, 2.90; N, 9.78. $C_{11}H_9F_3N_2O_2S$ requires C, 45.52; H, 3.12; N, 9.65%); ν_{max}(KBr)/cm^{-1} 3148, 3092, 1616; δ_H (200 MHz; DMSO-d_6) 1.33 (3H, t, J=7.0 Hz, CH_3CH_2), 4.06 (2H, q, J=7.0 Hz, CH_3CH_2), 7.11 (1H, dd, J=8.8, 2.4 Hz, C(5)H), 7.47 (1H, d, J=8.8 Hz, C(4)H), 7.60 (1H, d, J=2.4 Hz, C(7)H).

4.1.2. 6-Ethoxy-2-trifluorothioacetyliminobenzothiazoline (5). A mixture of **4** (0.40 g, 1.38 mmol) and Lawesson's reagent (0.33 g, 0.83 mmol) in toluene (20 mL) was kept at 110°C for 3 h (followed by TLC), after which it was cooled and the solvent evaporated. The solid yellow residue was flash chromatographed eluting with hexane/ethyl acetate (4:1) to afford **5** (0.41 g, 97%) as yellow plates. Mp 209–211°C (2-propanol). (Found: C, 43.21; H, 2.90; N, 8.98. $C_{11}H_9F_3N_2OS_2$ requires C, 43.13; H, 2.96; N, 9.14%); ν_{max}(KBr)/cm^{-1} 3146, 3076, 1492; δ_H (200 MHz; DMSO-d_6) 1.36 (3H, t, J=7.0 Hz, CH_3CH_2), 4.08 (2H, q, J=7.0, CH_3CH_2), 7.22 (1H, dd, J=9.0, 2.4 Hz, C(5)H), 7.55 (1H, d, J=9.0, C(4)H), 7.69 (1H, d, J=2.4 Hz, C(7)H).

4.2. Structure determination by X-ray crystallography

The X-ray analyses of **4** and **5** were carried out on a CAD-4 diffractometer using monochromated Mo K_α radiation (λ=0.71073 Å) at room temperature. Cell parameters were determined from 25 centered reflections using a standard procedure.[21] All data were corrected for Lorentz and polarization effects.[22] No absorption correction was applied to the intensities. The structures were solved with SIR97[23] and refined by full-matrix least-square methods using the SHELXL97 program.[24] All non-H atoms were refined anisotropically, except for the disordered atoms. The H atoms attached to nitrogen and oxygen atoms were found from a Fourier map, while all other H atoms were placed at idealized positions using standard geometric criteria and were treated as a riding model. The thermal ellipsoid plots and the computer-generated pictures were constructed with ORTEP III[25] and SCHAKAL[26]computer programs, respectively.

The crystals of **5** are very sensitive to solvent loss (2-propanol) and they were handled in protective oil. The transparent crystals showed fissures as soon as they were extracted from the crystallization solution and without protection they become opaque in a few minutes. So, a yellow crystal was selected and isolated in a glass capillary to keep it stable during the analysis. The three fluorine atoms were found to be disordered. Each atom occupies three alternative sites with occupancy of 40% for the first position and 30% for the second and third positions.

Crystallographic data for the structures reported in this paper have been deposited with the Cambridge Crystallographic Data Centre as supplementary publication no. CCDC-208333 (compound **4**) and CCDC-208334 (compound **5**). Copies of the data can be obtained from CCDC, 12 Union Road, Cambridge CB2 1EZ, UK (fax: int. code +44-1223-336-033; e-mail: deposit@ccdc.cam.ac.uk).

4.3. Computational studies

All calculations were performed with the Gaussian 98 program at the B3LYP/6-311G** level[27] with the default criteria implemented into the program. The molecular structures were initially optimized with the B3LYP/6-31G* method and then submitted to a complete geometry optimization under the C_s symmetry point group. For the isomers **7**, **8** and **11** the geometry was also optimized without any symmetry constraints in gas phase, chlorobenzene and ethanol. These solvent effects were taken into account by the Polarized Continuum (overlapping spheres) model[28] (PCM) with the proper solvent keyword within the Gaussian 98 program. Only the total electrostatic energy was considered, since the non-electrostatic contributions

were very similar (within 0.5 kJ/mol) for these isomers. The molecular mechanics (MM+) calculations were performed with the HyperChem 6.0 program[29] with the default parametrization and convergence criteria.

Acknowledgements

We gratefully acknowledge support for this work from the CNPq, FINEP, PADCT, CENAPAD-SP, PRONEX and RENAMI.

References

1. Minyaev, R. M.; Minkin, V. I. *Can. J. Chem.* **1998**, *76*, 776–787.
2. Ohkata, K.; Ohsugi, M.; Yamamoto, K.; Ohsawa, M.; Akiba, K. *J. Am. Chem. Soc.* **1996**, *118*, 6355–6369.
3. Barton, D. H. R.; Hall, M. B.; Lin, Z.; Parekh, S. I.; Reibenspies, J. *J. Am. Chem. Soc.* **1993**, *115*, 5056–5059.
4. Pandya, N.; Basile, A. J.; Gupta, A. K.; Hand, P.; MacLaurin, C. L.; Mohammad, T.; Ratemi, E. S.; Gibson, M. S.; Richardson, M. F. *Can. J. Chem.* **1993**, *71*, 561–571.
5. Kucsman, A.; Kapovits, I. In *Organic Sulfur Chemistry: Theoretical and Experimental Advances*; Bernardi, F., Csizmadia, I. G., Mangini, A., Eds.; Elsevier: Amsterdan, 1985; pp 191–245.
6. Burling, F. T.; Goldstein, B. M. *J. Am. Chem. Soc.* **1992**, *114*, 2313–2320.
7. Franchetti, P.; Cappellacci, L.; Grifantini, M.; Barzi, A.; Nocentini, G.; Yang, H.; O'Connor, A.; Jayaram, N. H.; Carrell, C.; Goldstein, B. M. *J. Med. Chem.* **1995**, *38*, 3829–3837.
8. Tanaka, R.; Oyama, Y.; Imajo, S.; Matsuki, S.; Ishiguro, M. *Bioorg. Med. Chem.* **1997**, *5*, 1389–1399.
9. Yamada, S.; Misono, T. *Tetrahedron Lett.* **2001**, *42*, 5497–5500.
10. Nagao, Y.; Hirata, T.; Goto, S.; Sano, S.; Kakehi, A.; Iizuka, K.; Shiro, M. *J. Am. Chem. Soc.* **1998**, *120*, 3104–3110.
11. Nagao, Y.; Iimori, H.; Goto, S.; Hirata, T.; Sano, S.; Chuman, H.; Shiro, M. *Tetrahedron Lett.* **2002**, *43*, 1709–1712.
12. Ángyán, J.; Poirier, R. A.; Kucsman, A.; Csizmadia, I. G. *J. Am. Chem. Soc.* **1987**, *109*, 2237–2245.
13. Hirata, T.; Nomiyama, J.; Sakae, N.; Nishimura, K.; Yokomoto, M.; Inoue, S.; Tamura, K.; Okuhira, M.; Amano, H.; Nagao, Y. *Bioorg. Med. Chem. Lett.* **1996**, *6*, 1469–1474.
14. (a) Hirata, T.; Shiro, M.; Nagao, Y. *Heterocycles* **1997**, *44*, 133–138. (b) Hirata, T.; Goto, S.; Tamura, K.; Okuhira, M.; Nagao, Y. *Bioorg. Med. Chem. Lett.* **1997**, *7*, 385–388.
15. Wexler, R. R.; Greenlee, W. J.; Irvin, J. D.; Goldberg, M. R.; Prendergast, K.; Smith, R. D.; Timmermans, P. B. M. W. M. *J. Med. Chem.* **1996**, *39*, 625–656.
16. (a) Pederson, B. S.; Lawesson, S.-O. *Tetrahedron* **1979**, *35*, 2433. (b) El-Barbary, A. A.; Clausen, K.; Lawesson, S.-O. *Tetrahedron* **1980**, *36*, 3309. (c) El-Barbary, A. A.; Lawesson, S.-O. *Tetrahedron* **1981**, *37*, 2641.
17. Cramer, C. J. Essentials of Computational Chemistry: Theories and Models; Wiley: New York, 2002.
18. St-Amant, A.; Cornell, W. D.; Halgren, T. A.; Kollman, P. A. *J. Comput. Chem.* **1995**, *16*, 1483–1506.
19. Allen, M. P.; Tildesley, D. J. Computer Simulation of Liquids; Clarendon: New York, NY, 1989.
20. Allinger, N. L. *J. Am. Chem. Soc.* **1977**, *99*, 8127–8134.
21. Enraf-Nonius, *CAD-4 EXPRESS*, Version 5.1/1.2; Enraf-Nonius: Delft, The Netherlands, 1994..
22. Spek, A. L. *HELENA: CAD-4 Data Reduction Program*; Utrecht University: Utrecht, The Netherlands, 1996.
23. Altomare, A.; Burla, M. C.; Camalli, M.; Cascarano, G.; Giacovazzo, C.; Guagliard, A.; Moliterni, A. G. G.; Spagna, R. *Sir97*: a new tool for crystal structure determination and refinement. *J. Appl. Crystallogr.* **1999**, *32*, 115–119.
24. Sheldrick, G. M. *SHELXL97: Program for the Refinement of Crystal Structures*; University of Göttingen: Germany, 1997.
25. Burnett, M. N.; Johnson, C. K. *ORTEP-III: Oak Ridge Thermal Ellipsoid Plot Program for Crystal Structure Illustrations*; Oak Ridge National Laboratory Report ORNL-6895, 1996..
26. Keller, E. *SCHAKAL99: A computer program for the graphic representation of molecular and crystallographic models*; Kristallographisches Institut der Albert-Ludwigs-Universität Freiburg: Germany, 1999.
27. Frisch, M. J.; Trucks, G. W.; Schlegel, H. B.; Scuseria, G. E.; Robb, M. A.; Cheeseman, J. R.; Zakrzewski, V. G.; Montgomery Jr., J. A.; Stratmann, R. E.; Burant, J. C.; Dapprich, S.; Millam, J. M.; Daniels, A. D.; Kudin, K. N.; Strain, M. C.; Farkas, O.; Tomasi, J.; Barone, V.; Cossi, M.; Cammi, R.; Mennucci, B.; Pomelli, C.; Adamo C.; Clifford, S.; Ochterski, J.; Petersson, G. A.; Ayala, P. Y.; Cui, Q.; Morokuma, K.; Malick, D. K.; Rabuck, A. D.; Raghavachari, K.; Foresman, J. B.; Cioslowski, J.; Ortiz, J. V.; Baboul, A. G.; Stefanov, B. B.; Liu, G.; Liashenko, A.; Piskorz, P.; Komaromi, I.; Gomperts, R.; Martin, R. L.; Fox, D. J.; Keith, T.; Al-Laham, M. A.; Peng, C. Y.; Nanayakkara, A.; Challacombe, M.; Gill, P. M. W.; Johnson, B.; Chen, W.; Wong, M. W.; Andres, J. L.; Gonzalez, C.; Head-Gordon, M.; Replogle, E. S.; Pople, J. A. *GAUSSIAN 98* (Revision A.9); Gaussian, Inc.: Pittsburgh, PA, 1998..
28. Miertus, S.; Scrocco, E.; Tomasi, J. *Chem. Phys.* **1981**, *55*, 117–129.
29. HyperChem Release 6.0. Hypercube, Inc.: Gainesville, FL, 1999.